DISPLACEMENTS AND EARTH PRESSURE AT INTEGRAL BRIDGES AND COMPARISON OF DIFFERENT CONSTRUCTIONS FOR THE BACKFILL AREA

S. Szczyrba & W. Kudla
Institute of Mining Engineering and Special Foundation Engineering
TU Bergakademie Freiberg, Germany
Sebastian.Szczyrba@mabb.tu-freiberg.de

ABSTRACT

During the last years integral bridges have been build more frequently in Germany since the costs of construction and maintenance can be reduced. At these bridges the earth pressure at the abutments is influenced by the thermal induced changes of the bridge's length, which has to be considered during the design.

At an integral motorway bridge with spread footings near Frankfurt/Germany the earth pressure, temperatures and displacements were recorded since March 2008 at four different types of backfilling.

During the present observation time the temperature had varied in the middle of the bridge deck between 30 °C and -6 °C. At the backfill area with a coarse grained soil the resulting earth pressure had varied between 120 kN/m in winter and 500 kN/m in summer. With a vertical layer of EPS-foam in an other backfill-area the earth pressure could be reduced down to 150 kN/m² with less seasonal changes.

The settlements at the road surface caused by traffic have been relatively small since traffic release. The unevenness of the road surface in the longitudinal profile was dominated by the state of the road surface before traffic release.

1. PROBLEM STATEMENT

Integral bridges are characterised by monolithically linked bridge superstructures and abutments as well as by piles if applicable. Therefore, the assembly of bearings and expansion joints can be waived. However, temperature fluctuations cause imposed strains in the supporting structure which must be considered during the design.

In case of sufficiently bearing ground, integral bridges in Germany are normally erected in shape of a framework construction with shallow foundations [2]. Besides bridges of reinforced or prestressed concrete, composite steel structures are increasingly used [5].

One advantage of framework structures is the better utilisation of cross-sections. This significantly helps reducing the mid-span moment in the bridge superstructure by means of the corner moment, which in turn facilitates reduced construction height of the superstructure or increased spans at the same superstructure height.

The seasonal temperature fluctuations as well as the fluctuation of ambient temperature during the day lead to length changes in the bridge superstructure, which are carried over to the abutments (Figure 1). This causes displacements between the abutment and the adjacent backfill area, which generates changes of the earth pressure affecting the abutments [11]. Consequently, the earth pressure may fall down to the active earth

pressure in winter position, whereas earth pressure arising in summer may reach rates well beyond the at-rest earth pressure. The changing strain imposed by earth pressure must therefore be considered realistically already during design [1,6,7].

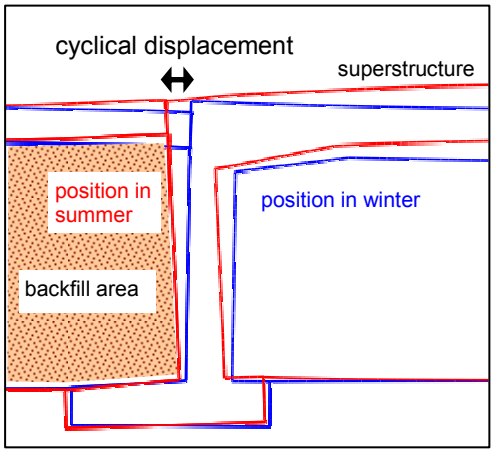

Figure 1 – Cyclical displacements of the abutment between summer and winter

In the course of a research project, multi-annual measurements at a frame bridge near Frankfurt/Main, Germany, were carried out with the focus on earth pressure, temperature and horizontal displacement of the abutments. In addition, the vertical deformations at the road surface (i.e. the settlement) were also measured, since the cyclical displacement of the abutments toward the backfill area may cause uplift at the road surface, and even more likely settlement due to increasing lateral compression of the backfill material [3].

The measurements were part of a research project, with the main aim to reduce the settlements in the backfill area. Therefore different types of backfilling were carried out at two motorway bridges. The structures were one conventionally built bridge consisting of a single-span girder with bearings and expansion joints and one frame bridge with shallow foundations (see [8]). In total, eight different kinds of backfill material were applied at the two bridges and the settlement at the road surface under live traffic conditions was monitored for a period of up to four years.

This article presents the measurement results at the integral frame bridge, where four different kinds of backfilling were performed. The measurements carried out at the conventional bridge are outlined in [10].

2. DESCRIPTION OF THE STRUCTURE

The analysed structure BW 15 was newly erected as a replacement at the federal motorway A66 between Frankfurt/Main and Wiesbaden in 2007/2008. It features a clearance of 17.5 m and was carried out as a reinforced concrete frame with shallow foundations. The abutments have a height of 7.5 m. With a crossing angle between the axes of 45°, the structure shows a great skewness (see site plan in Figure 2). The motorway A66 crosses the bridge with three lanes in each direction and one hard shoulder. The structure's total width including the edge beams is 34 m. The ground at the site consists of gravel with a high bearing capacity.

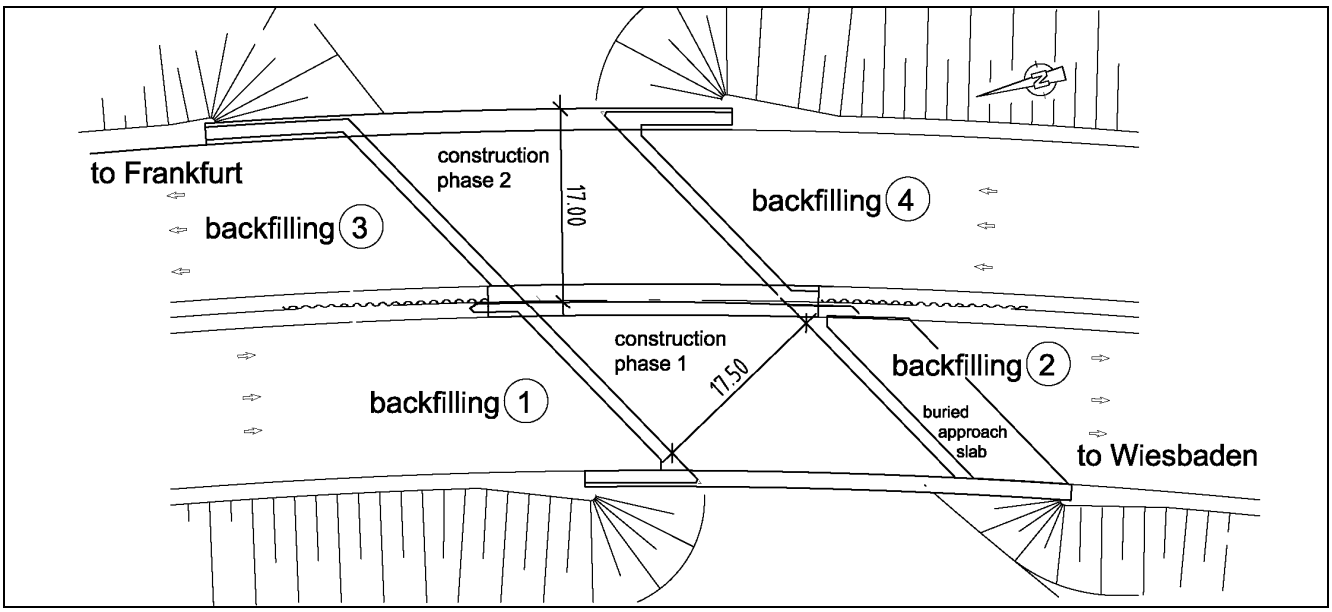

Figure 2 – Site plan of structure BW 15 at motorway A66 between Frankfurt/Main and Wiesbaden

Between the lanes in each direction, the bridge is divided by joints, i.e. a separate bridge part for each direction was erected in two sequential construction phases. With the support by the Hessian Road And Traffic Administration, four backfilling methods listed in Table 1 and Figure 3 were carried out at this structure.

During the first construction phase between August 2007 and March 2008, the roadway toward Wiesbaden was extended to three lanes while traffic was entirely led over the roadway in the direction of Frankfurt.

Backfill area 1 was built as a reference case according to the corresponding German guidelines with a coarse grained soil, which consists of approximately 40 % gravel, 55 % sand and less than 5 % fine grain with a diameter less than 0.06 mm. The material was implemented with a degree of compaction D_{Pr} of at least 100% of the standard Proctor density (Figure 3). Frame shear tests carried out with earth-moist material yielded a friction angle φ' of 35° and a cohesion c' of 14 kN/m². Static plate bearing tests on the subgrade and within the backfill material yielded deformation moduli E_{V2} at the second loading between 78 MN/m² and 149 MN/m² for the coarse-grained soil at an average magnitude of 92 MN/m² (Table 2).

Table 1 – Performed types of backfilling

Backfilling 1	coarse-grained soil according to the corresponding German guidelines [4] as a reference case
Backfilling 2	buried approach slab at the top edge of the backfill area
Backfilling 3	cement-improved fine-grained soil and vertical EPS foam layer to reduce earth pressure
Backfilling 4	cement-improved coarse-grained soil and vertical EPS foam layer to reduce earth pressure

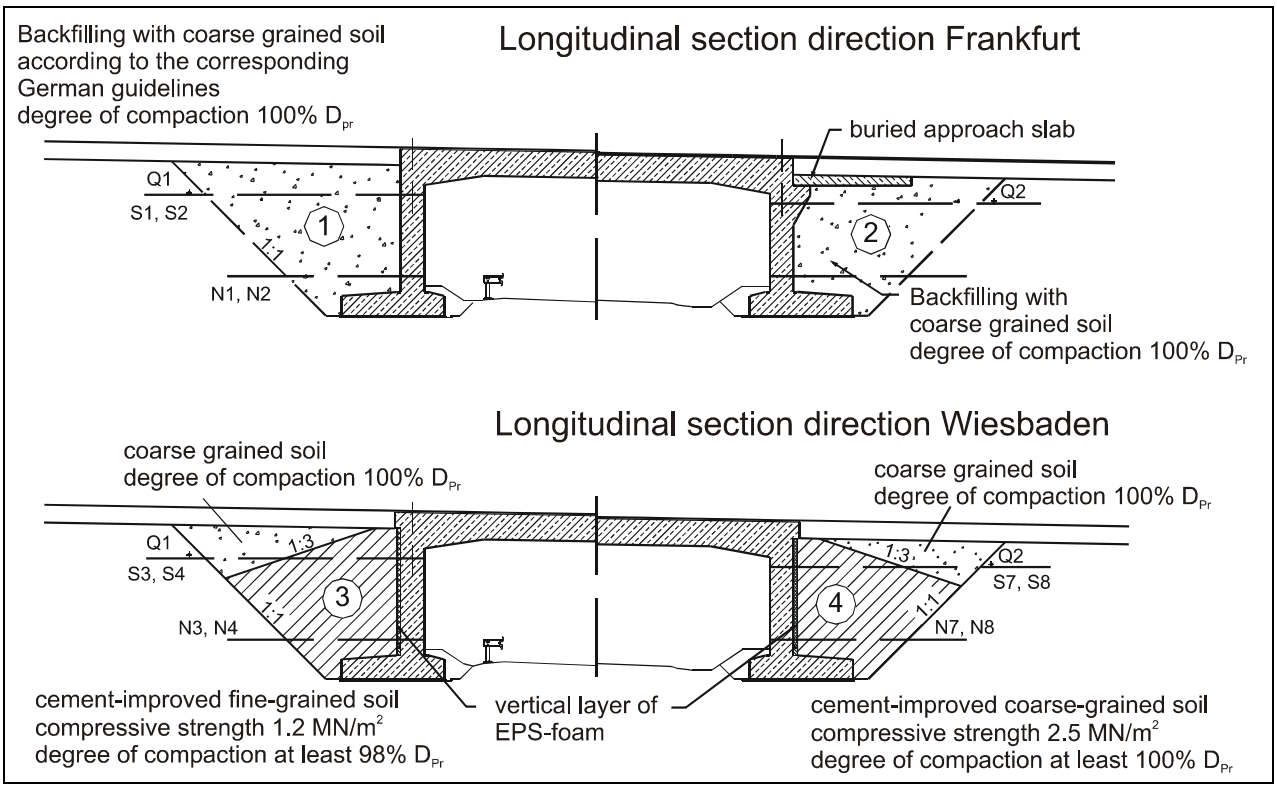

Figure 3 – Longitudinal section with monitoring program at structure BW 15
(S … Length and inclination measuring tube, N … Inclination measuring tube)

In backfill area 2 a buried approach slab was implemented at the junction of bridge structure and backfill material. The slab surface was located in the height of the formation (Figure 4). Subsequently, the usual road structure with a height of 0.9 m was applied upon the approach slab.

At the abutment, a 0.85 m wide reinforced concrete bracket was produced as a bearing for the approach slab. The approach slab stretches in parallel with the abutment and is 6.00 m wide, with the average thickness of the slab being 0.5 m. The roadway toward Wiesbaden could be opened to traffic in March 2008.

Figure 4 – Buried approach slab at backfill area 2

Table 2 – Check test results

	Coarse-grained soil	Cement-improved fine-grained soil	Cement-improved coarse-grained soil
Degree of compaction (standard Proctor density)	100 - 104% D_{Pr}	98% D_{Pr}	100% D_{Pr}
Deformation modulus E_{v2} (static plate bearing test)	92 MN/m²	184 MN/m² (28 days after implementation)	600 MN/m² (28 days after implementation)
Monoaxial compressive strength	--	1.12 to 1.34 MN/m² (age of sample 28 days)	2.48 to 2.89 MN/m² (age of sample 28 days)
Shearing strength	Friction angle φ' = 35° Cohesion c' = 14kN/m²	--	--

During the second construction phase, two wedges with cement-improved soil were made in backfill area 3 and 4. The source material in area 3 consisted of fine-grained soil with a fine-grain share (d ≤ 0.06 mm) of approx. 35 %, whereas area 4 featured coarse-grained soil with a fine-grain share of approx. 8 %. In order to avoid growing imposed strain at the bridge frame due to the significantly higher shearing strength and the higher deformation resistance of the cement-improved soil, a 20 cm thick vertical EPS rigid foam layer was implemented at the abutment wall, the upper edge of which forming a 30 cm wide projection of the bridge superstructure.

The soil-binder mixture was produced in place at a separate mixing site. To achieve this, cement was scattered across the spread layers of compressed source material and tilled under (Figure 5), immediately followed by implementation into the backfill area.

The amount of binder was determined during suitability tests in such a way that the prescribed compressive strength of 1.2 MN/m² in area 3 and 2.5 MN/m² in area 4 could be kept. During implementation, this was also confirmed by means of samples that were made from the mixed-in-place material (see Table 2). Static plate bearing tests in both backfill materials could be carried out 28 days after implementing the soil-binder mixture. The resulting deformation moduli E_{V2} were 184 MN/m² at the fine-grained source material in area 4 and 610 MN/m² at the coarse-grained material in area 4.

Figure 5 – Production of the soil-binder mixture for soil improvement

In order to guarantee a steady transition to the adjacent road sections, the surface of the cement-improved soils was formed with an inclination of 1:3 (see Figure 3). Above, the same coarse-grained material as in backfill area 1 and 2 was applied. The roadway toward Frankfurt could be opened to traffic in December 2008.

3. MEASUREMENT PROGRAMME

Earth pressure measurements were carried out at backfill area 1 with coarse-grained soil and at backfill area 3 with cement-improved soil. In each roadway axis, a section with eight earth pressure cells at various levels was installed with the cells positioned in pairs in order to be able to check the measured readings as well as to have a redundant system (Figure 6). Additional cells were aligned at a depth of 2.3 m in order to survey earth pressure differences in both the obtuse-angled and the acute-angled corner of the framework.

At backfill area 1, the earth pressure cells were attached directly to the abutment wall. During the following implementation of each fill layer, sand was applied to the immediate contact area of a cell and the material was gently compressed with a tamper. On the opposite, the earth pressure cells at backfill area 3 with the cement-improved soil were implemented between the EPS layer and the abutment by making precisely fitting recesses in the EPS layer.

The displacements between abutment and backfill area were captured with one triple extensometer each, consisting of three plastic rod extensometers with lengths of 1.2 m; 2.5 m and 5.0 m at backfill area 1. At the triple extensometer in backfill area 3, which was implemented during the second construction phase, the lengths of every extensometer were reduced due to the high solidity of the cement-improved soil (Figure 6).

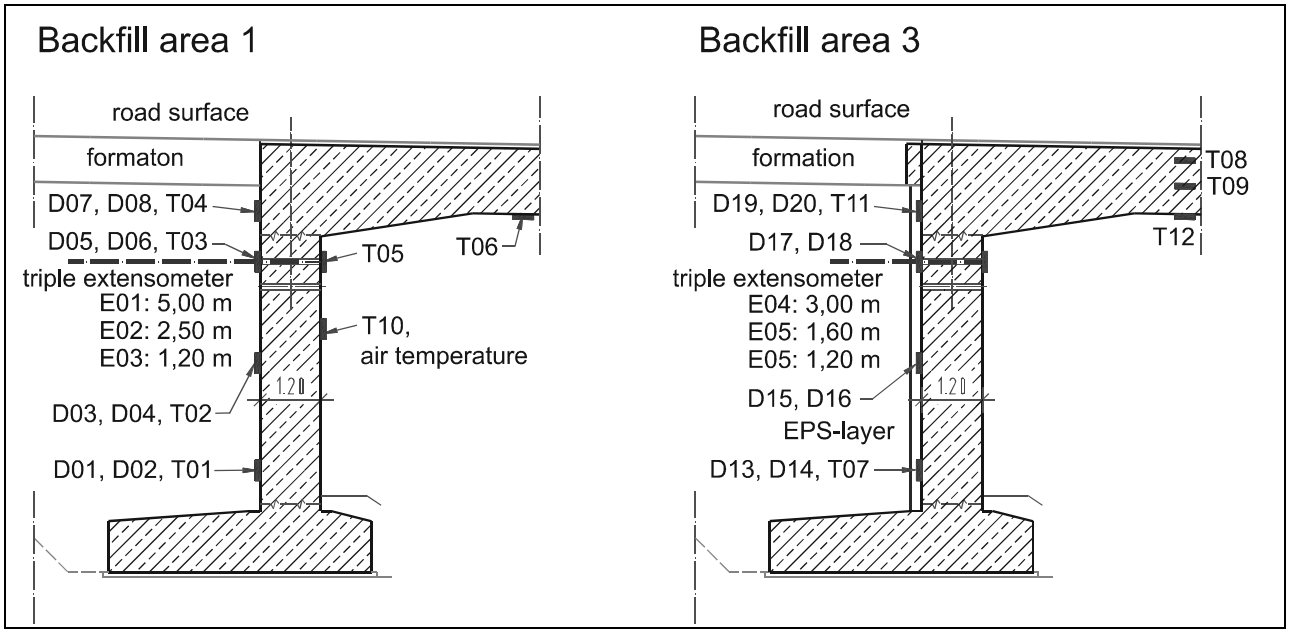

Figure 6 – Measurement sections at backfill area 1 and 3 with earth pressure cells D, temperature sensors T and extensometers E

In order to capture the settlements within the backfill material under traffic conditions, horizontal measuring tubes for inclinometer measurements were aligned at various levels inside the backfill material (see Figure 3). The lower position of inclination measuring tubes is approx. 6.4 m below the road surface. The upper length measuring tubes run approx. 4.0 m above the lower inclination measuring tubes (2.4 m below the road surface). Along with capturing vertical deformation, the length measuring tubes also allow the measuring of the longitudinal deformation between the single 1 m long tube sections. Deformation at the road surface was captured by means of levelling.

4. MEASUREMENT RESULTS

4.1. Temperature profile

The measurements allowed to capture the temperatures at the structure over a period of almost three years. The air temperatures taken hourly by the sensor T10 made up between -12 °C in winter and 33 °C in summer, with a daily fluctuation of up to 17 °C. The overall survey period yielded an average air temperature of 11 °C at the bridge site. In spite of various temperature profiles during every month, all three years saw approximately the same maximum temperatures in summer and minimum temperatures in winter.

Sensor T9 was attached to the reinforcement and set in concrete during construction of the bridge superstructure, so that this sensor captures the temperature profile in the centre of the bridge superstructure (Figure 6). The temperature in the middle of the superstructure lay between -6 °C and 31 °C, making up a seasonal fluctuation of a maximum 37 °C between summer and winter. Figure 7 shows the daily mean temperatures of both sensors.

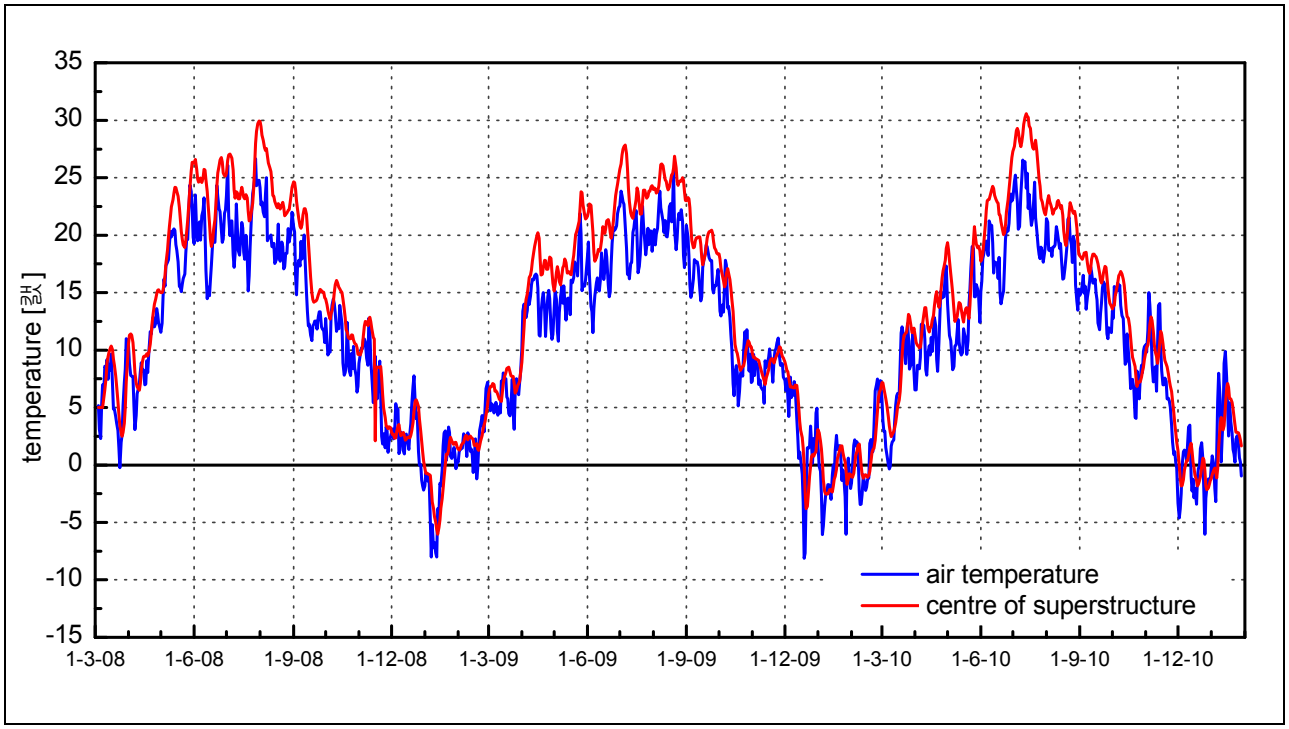

Figure 7 – Air temperature and temperature in the bridge superstructure's centre (daily mean temperature), between March 2008 and February 2010

The bridge centre temperature correlates strongly with the average air temperature of the previous six days according to equation 1. For this, the approach according to equation 2 with a coefficient of determination $R^2 = 0.99$ could be established.

$$\overline{T}_{air}^{6d}(t) = \tfrac{1}{6d} \sum_{t=-6d}^{t} \overline{T}_{air}^{1d}(t) \qquad /1/$$

$$T_{centre} = \begin{cases} \overline{T}_{air}^{6d}(t) & if\ \overline{T}_{air}^{6d}(t) < 0°C \\ 1{,}2 \cdot \overline{T}_{air}^{6d}(t) & if\ \overline{T}_{air}^{6d}(t) \geq 0°C \end{cases} \qquad /2/$$

$\overline{T}_{air}^{6d}(t)$ … average measured temperature of previous six days

$\overline{T}_{air}^{1d}(t)$ … measured daily mean air temperature (sensor T10)

T_{centre} … temperature at bridge centre (sensor T9)

At temperatures below 0°C in winter, the temperature at the bridge superstructure corresponded directly to the average air temperature of the previous six days. At temperatures above zero, the superstructure is additionally warmed by solar radiation, which raised the superstructure's inside temperature by 20% beyond the average air temperatures of the previous six days.

4.2. Displacement of the abutments

The displacement of the entire bridge structure could be captured by geodetic position measurements carried out in both summer and winter. For this purpose, every abutment has six target signals and eight fixed-point piers as reference points aligned in a distance of 30 to 100 m from the bridge. Due to the considerable skew angle of 45° of both bridge structures, deformation at the superstructure's acute-angled corner was significantly stronger than at the obtuse-angled corner.

The bridge superstructure's total deformation was made up by the shares of temperature deformation, shrinkage deformation and rigid body displacement of the entire structure. In order to determine the size of each share, the elongations $\varepsilon_{T+cs} = \Delta L/L$ between the measuring markers facing each other transversely below the bridge superstructure were analysed first, depending on the average temperature inside the superstructure. At temperature fluctuations of 22 K, elongation between the measurements in winter and summer 2010 averaged at $\varepsilon_T = 0.21$ mm/m. This allowed to establish a temperature coefficient of $\alpha_T = 0.95 \cdot 10^{-5}\ K^{-1}$ for the bridge superstructure's concrete, which corresponds well with the usual approach of $\alpha_T = 1.00 \cdot 10^{-5}\ K^{-1}$. The measurements in spring 2008, winter 2009 and winter 2010 was carried out at nearly the same temperatures (difference of the temperature between the measurements of maximum 4°C). This allowed to determine the magnitude of the shrinkage stress ε_{cs} in this period of time, which amounted to -0.3 mm/m after 2.4 years at the bridge erected in the first construction phase and to -0.1 mm/m after 1.6 years at the bridge erected in the second construction phase. The different shrinkage shortenings were caused by the different completion dates in spring/early winter 2008.

Position measurements at the abutments of the bridge built in the first construction phase brought to evidence that, along with the cyclical temperature deformations and constant shrinkage shortenings, rigid body displacement of the entire structure had also taken place.

Due to the soldier pile wall for erecting the Frankfurt-bound roadway bridge, less resistance against horizontal force transmission was encountered at the Wiesbaden-facing abutment than at the Frankfurt-facing one. This meant a stronger displacement of the Wiesbaden-facing abutment and consequently a rotation of the entire structure around the south-western corner with a rotation angle of approx. $5 \cdot 10^{-5}$ rad, so that the structure's opposite acute-angled corner had been displaced by approx. 2 mm to the southeast (see Figure 8).

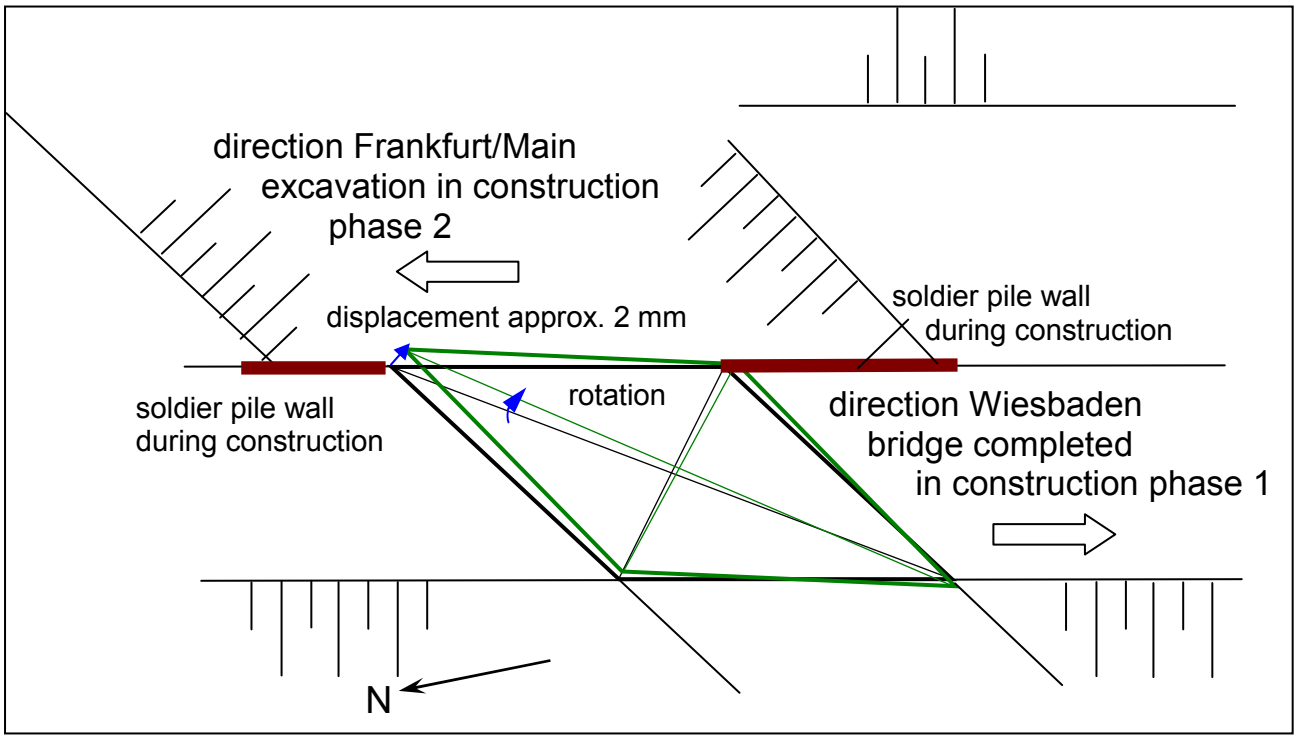

Figure 8 – Rotation and displacements of the bridge in the direction to Wiesbaden during construction phase 2 with the excavation in the direction to Frankfurt (not to scale)

The position measurement was carried out two times a year for capturing the structure's total displacement. Deformations between the backfill area and the abutments with earth pressure measurement were additionally determined by extensometers aligned 2.3 m below the road surface with a length of 5 m at backfill area 1 with its coarse-grained soil. Deformations at extensometer E01 amounted to 2.7 mm between the minimum and maximum readings in winter/summer, while the deformations due to rotation of the abutment were stronger toward the air-side face (Figure 9). The comparison of the extensometer measurement results with the outcomes of position measurements revealed that approx. 70% of the total deformation could be determined by means of the 5 m long extensometers E01. The deformations of the 2.5 m long extensometer E02 were roughly half as large as those at extensometer E01.

At backfill area 3 with the cement-improved soil and the vertical EPS layer for earth pressure reduction, most of the deformations were absorbed by the EPS layer, so that the extensometers E04 and E05 yielded almost equal measurement results, with deformations amounting to approx. 2.4 mm between winter and summer.

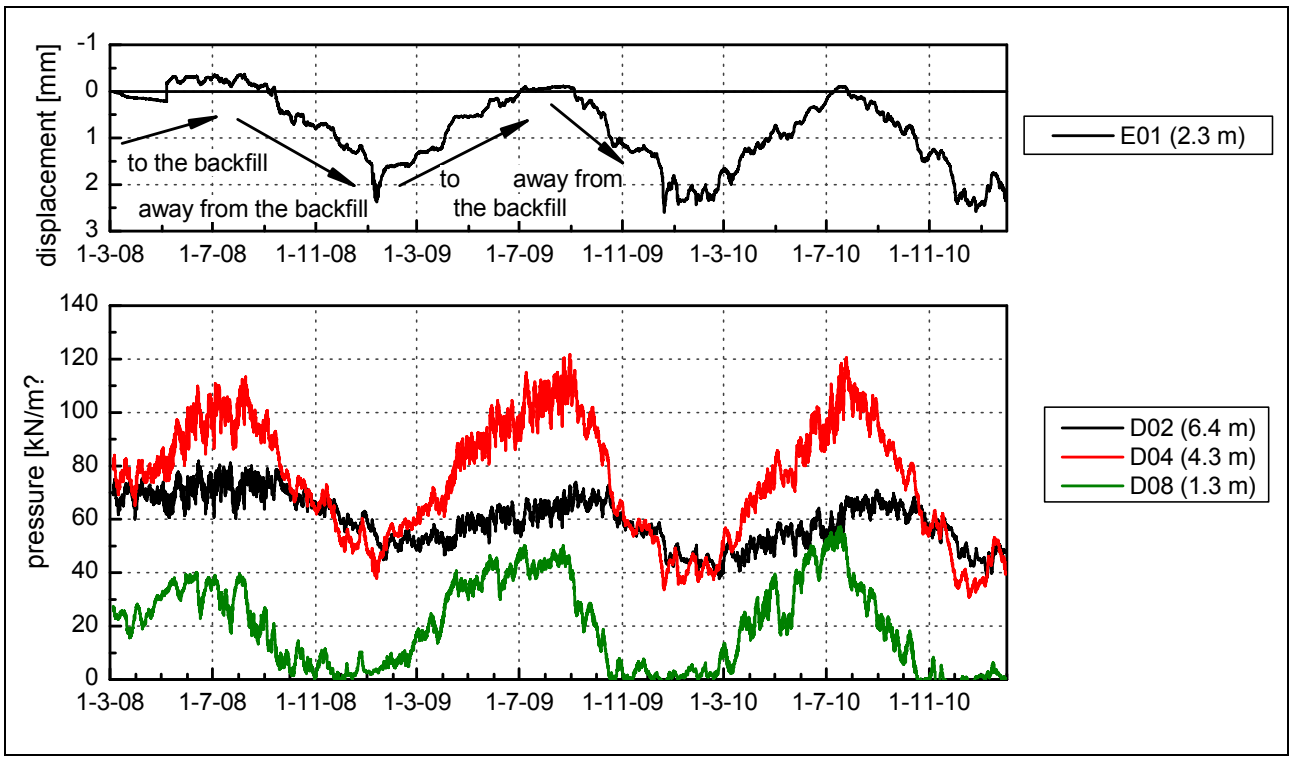

Figure 9 – Displacements and earth pressures at selected sensors in backfill area 1 between March 2008 and February 2010

5. EARTH PRESSURE PROFILE AT STRUCTURE BW 15

The abutments' displacement toward the backfill material in backfill area 1 with coarse-grained soil caused considerable earth pressure fluctuations between summer and winter, which were additionally superimposed by distinctive daily fluctuations. In this process, the greatest seasonal fluctuations in earth pressure were recorded at the earth pressure cells D03 and D04, situated 4.3 m below the road surface (approximately half of the abutments' height). The readings lay between 120 kN/m² in summer and 40 kN/m² in winter at sensor D04 (figure 6 and 9). The biggest daily fluctuations were encountered in summer and amounted to as much as 20 kN/m². At earth pressure sensor D08, situated 1.3 m below the road surface, the maximum earth pressure recorded so far during the past three years was 60 kN/m² and was therefore higher than the vertical stress, which amounted to only approx. 30 kN/m² due to the cells small depth below the road surface. With the temperatures declining every autumn, the earth pressure at the upper cells decreased in a way that cell D08 sensed almost no earth pressure between November and March (fig. 9). Therefore, the ratios K of horizontal and vertical stress fluctuate between $K_{min.D08}$ = 0 in winter and $K_{max.D08}$ = 2.0 in summer at cell D08. Hence, earth pressure readings encountered at this cell lay clearly beyond the at-rest earth pressure of K_0 = 0.4 (K_0 = 1-sin φ'). Comparison of the summer maxima also shows an increase of the maximum earth pressure in summer at almost equal displacement rates and temperatures, at all cells, in which earth pressure decreased in winter to 0 kN/m² (D05, D06, D07, D08).

Significant earth pressure fluctuations were also seen at the cells D01 and D02 positioned at a depth of 6.4 m and thus only 0.8 m above the upper edge of the foundations (Figure 6). The earth pressure recorded there lay between 40 kN/m² in winter and 80 kN/m² in summer (see Figure 9). However, the maximum readings in summer decreased steadily during these three years.

The range of earth pressures encountered at the earth pressure cells in backfill area 1 with coarse-grained soil was entered into Figure 10, using the average readings of the respective pair of cells. For a better comparison, Figure 10 additionally includes the at-rest earth pressure profiles as well as the passive and active earth pressure profiles.

The analysis of large-scale model tests and measurements at lock chamber walls allowed VOGT [12] to establish an empirical relationship describing a correlation between a mobilised earth pressure coefficient K_{mob}, and the displacements $s_h(z)$ for every single spot of a wall at a depth z. In Germany, this approach is used for the calculation of integral bridges [9].

$$K_{mob}(z) = K_0 + (K_{ph} - K_0) \cdot \frac{v_h(z)/z}{a + v_h(z)/z} \qquad /3/$$

K_{mob} … Coefficient for mobilised earth pressure at depth z
K_0 … Coefficient for at-rest earth pressure
K_{ph} … Coefficient for passive earth pressure
$v_h(z)$ … Horizontal displacement at depth z
z … Depth below road surface
a … Coefficient for compressed sand a = 0.01

The position measurement at the abutment pointed to a rotation of the abutment around a centre of rotation at the depth of the foundation's lower edge between summer and winter position. With the centre of rotation situated approximatly H = 8.5 m below the road surface and with an abutment's head displacement of approx. $v_h(0m)$ = 4mm between summer and winter, a rotation angle $v_h(0m)/H$ of roughly 0.0005 could be determined. This allowed establishing the horizontal deformations $v_h(z)$ across the entire height of the abutment. The profile of the mobilised earth pressure e_{mob} calculated according to equation /3/ at summer position is also displayed in Figure 10. With this approach, the upper and lower measurement results could be depicted well. However, the measurement results from the centre lay clearly above the mobilisation graph.

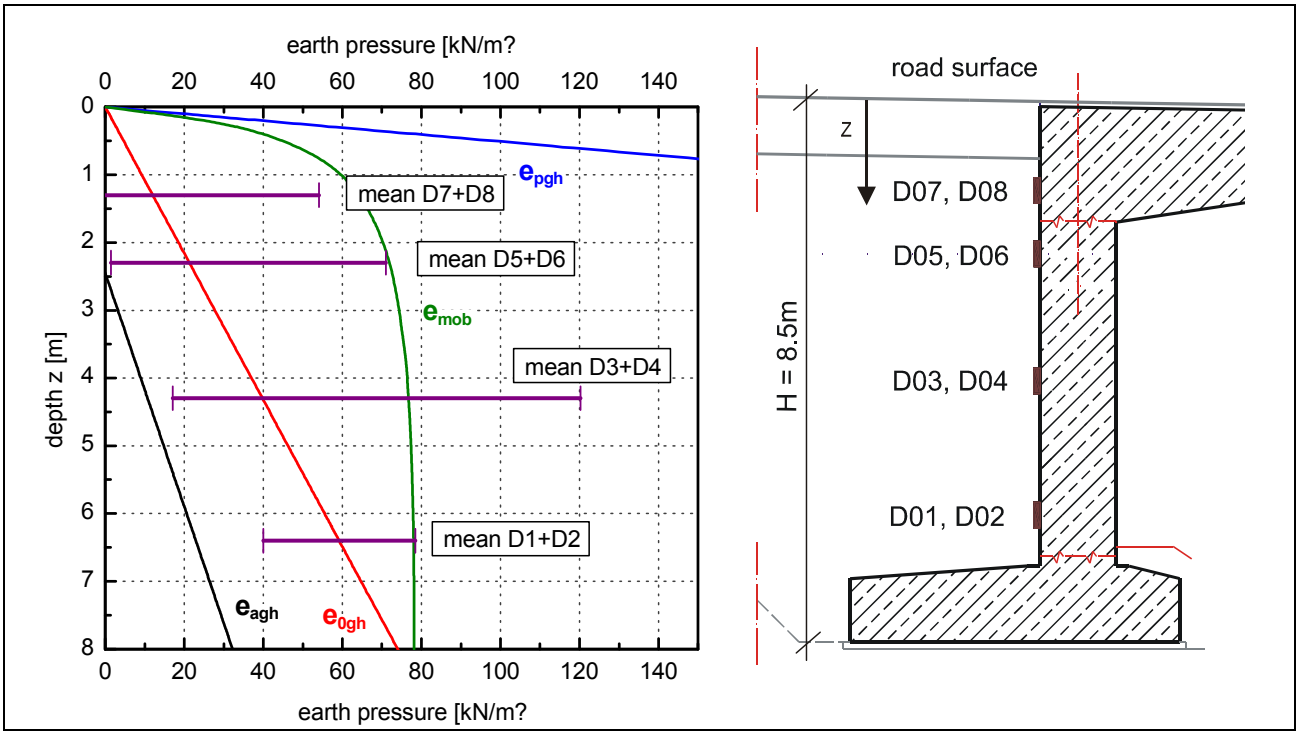

Figure 10 – Earth pressure at backfill area 1 with coarse-grained soil and comparison with theoretical earth pressure approaches

When calculating the winter position, it is important to consider a lower limiting value of the active earth pressure that was determined in Figure 10, taking the cohesion into account. The influence of cohesion led to no earth pressure being measured at the upper abutment area in the winter half year, which corresponded very well with the theoretical values. The lower-placed cells yielded earth pressures above the active earth pressure, since the horizontal deformations at this depth were smaller and hence the effective earth pressure did not fall down to the active earth pressure's limiting value.

Both the maximum and minimum earth pressures encountered so far at backfill area 1 with the coarse-grained soil are displayed in figure 10. It turned out however that the upper area showed an increase of the maximum values between the summers of the previous three years, whereas the maximum summer earth pressure at the lower cells decreased. Therefore, the total resulting earth pressure E_{res} acting upon the abutment cannot be determined directly from Figure 10. Hence, daily mean values were gained from the respective measurement results and the resulting earth pressure E_{res} was calculated according equation /4/. Figure 11 shows the resulting earth pressures E_{res} taking into account the temperature in the centre of the bridge structure.

$$E_{res}(t) = \int_z \sigma_h(z,t)\,dz \qquad /4/$$

$E_{res}(t)$ … resulting earth pressure in the measurement cross-section at the time t
$\sigma_h(z,t)$ … measured earth pressure in the depth z at the time t

In the measurement cross-section at backfill area 1 with coarse-grained soil, the resulting earth pressure E_{res} in summer amounted to maximum 493 kN/m at superstructure temperatures of 30 °C. According to Vogt's approach, a resulting earth pressure of 565 kN/m at summer position was determined, which lay 15 % above the measurement results. Hence, this approach is sufficiently precise for calculating when assuming the displacements between winter and summer position as input values. Due to the cyclical daily fluctuations appearing in addition to the seasonal fluctuations, rearrangements take place in the grain skeleton and the acting earth pressure emerges after several years independently of the abutments' initial position.

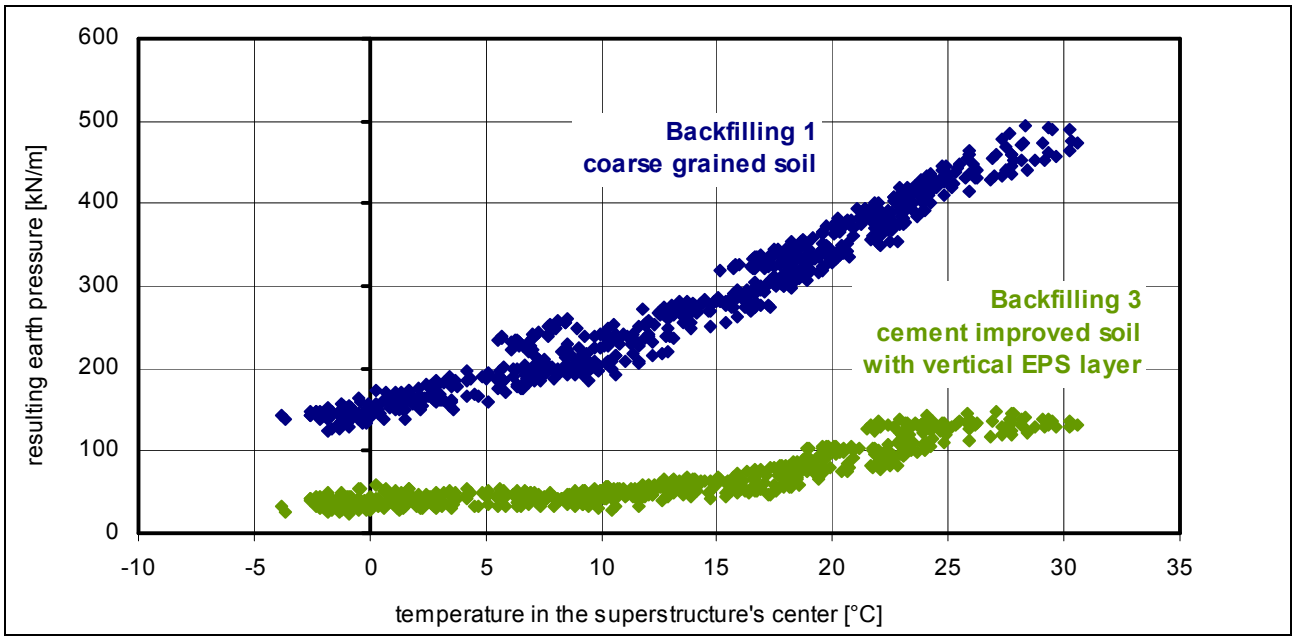

Figure 11 – Resulting earth pressure at the measurement cross-sections depending on the temperature

The examined frame structure proves to be a relatively small one with a span of 17.5 m and thus shows only relatively small horizontal displacements of approx. 4 mm at the abutments' upper edge due to temperature deformations. However, these comparatively small deformations led to a very strong decrease of the resulting earth pressure E_{res} at winter position down to 124 kN/m in winter 2010/2011 at superstructure temperatures of -2 °C.

For a better comparison, the ratios K were formed between the resultant force of earth pressure E_{res} and the resultant force E_{vert}, which was calculated by means of a hydrostatic approach of vertical stress due to the self-weight across the total height of the abutment $E_{Vert} = \frac{1}{2}\gamma h^2$. The winter ratios were K_{winter} = 0.23 and climbed up to the fourfold in summer with K_{summer} = 0.93.

At backfill area 3, a vertical EPS layer was implemented between the abutment and the cement-improved soil with a compressive resistance of approx. 1.2 N/mm² to significantly reduce earth pressure acting upon the abutment. The ranges of the measured earth pressures were spread across the entire height of the abutment relatively equally, as figure 12 shows. In winter, the resulting earth pressure declined down to 25 kN/m, but reached as much as 157 kN/m in summer (Figure 11). This allowed to prove that a targeted reduction of the earth pressure by applying a vertical EPS layer to the abutment's back is possible.

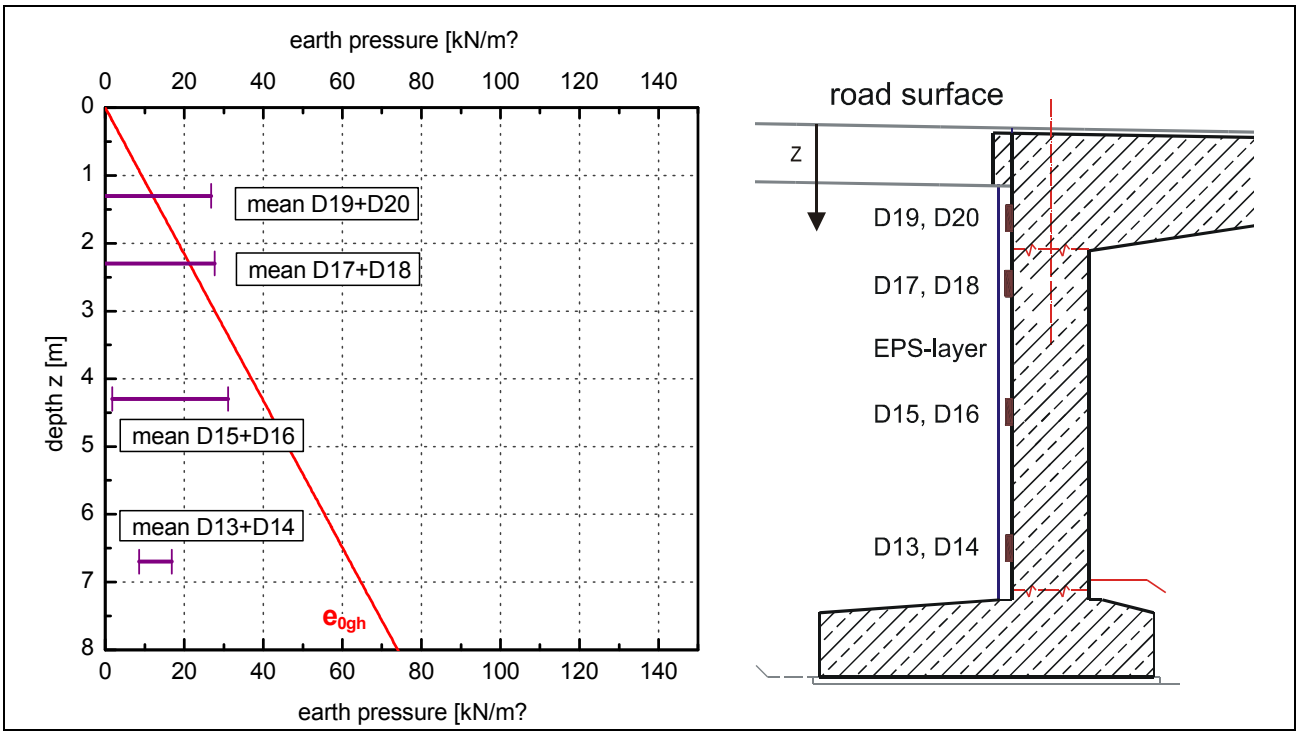

Figure 12 – Earth pressure at backfill area 3 with cement improved fine-grained soil and a vertical layer of EPS foam

6. EVENNESS OF THE ROAD SURFACE

The road's evenness in the longitudinal profile influences travel comfort and safety as well as the stress on vehicles and goods. For construction, an even nominal height of the road surface with large vertical curvature radii is prescribed. Height inaccuracies during production of the road surface layers and due to settlement during the following period of utilisation can cause surface irregularities. In order to estimate the magnitude of these two main issues, the height of the road surface was determined by levelling after implementation and with an interval of six months over a period of two years after traffic release.

Divergences during construction were determined by height differences between the prescribed nominal height and the actual height, which was measured by levelling prior to opening to traffic. The readings varied between +10 mm and -18 mm in larger sections, while increases of up to +30 mm were found in some partial areas. Figure 13b shows the divergences between nominal and actual heights found at the example of the Frankfurt-bound roadway prior to opening to traffic and during subsequent measurements.

The settlements after opening to traffic depicted in figure 13a were considerably smaller than the divergences during construction and amounted to only a few millimetres. The biggest deformations with a size of approx. 6 mm were found at the middle of the bridge between the measurements in summer and winter and were caused by temperature deformations of the bridge superstructure. After opening to traffic, settlements above backfill area 1 with the coarse-grained soil amounted relatively equally to 4 mm. Settlements above the approach slab at backfill area 2 were slightly smaller (3 mm), yet increased significantly to 5 mm directly behind the approach slab. Settlements in the areas 3 and 4 with the cement-improved soil lay between 2 and 3 mm after opening to traffic.

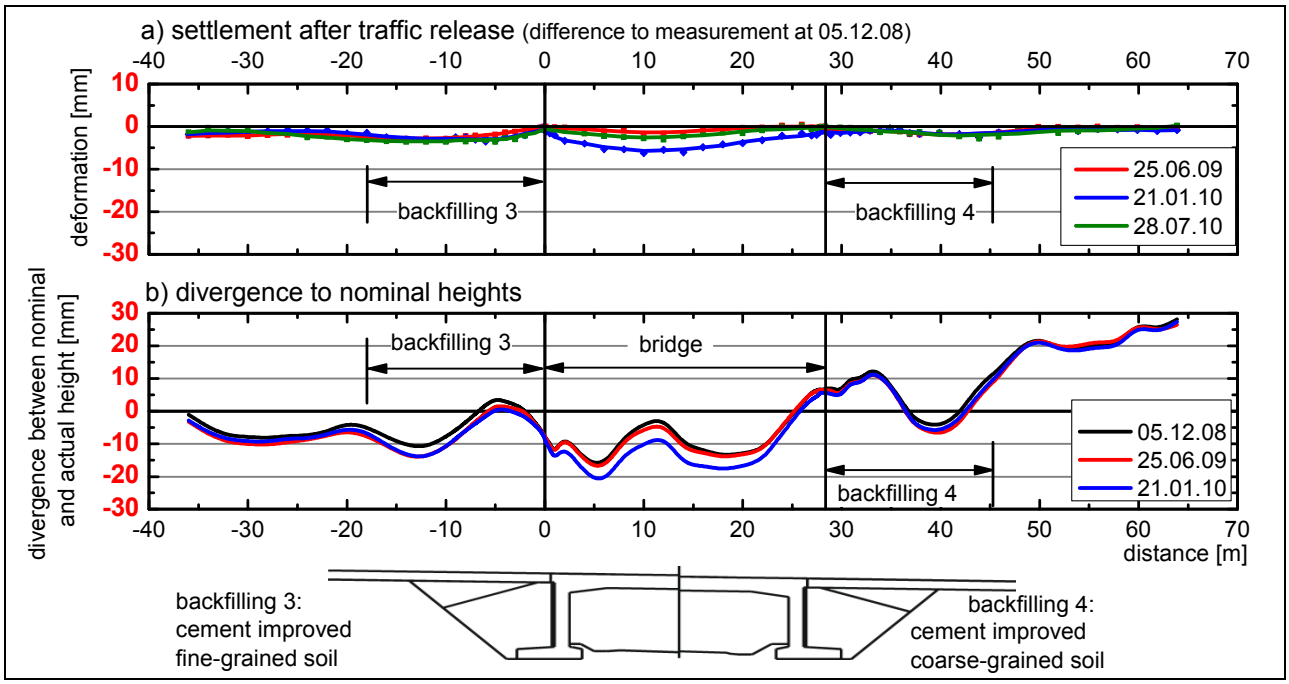

Figure 13- Levelling of road surface on Frankfurt-bound hard shoulder,
a) Settlements after opening to traffic
b) Divergence of measured actual heights from set height
(measurements prior to and after opening to traffic)

7. SETTLEMENTS INSIDE THE BACKFILL MATERIAL

Settlements inside the backfill material could be captured by inclinometer measurements at horizontal inclination meter tubes positioned within the backfill material at two different heights.

Since the settlements at the road surface were already very small, only deformations up to 2 mm were encountered within the various backfill areas. At the lower measureing tubes however, settlement measurements could be performend also during construction, which yielded additional settlements of approx. 2 mm. These settlements occurred during construction prior to finishing the road surface and therefore had no influence on the road's evenness in the longitudinal profile.

CONCLUSIONS

Abutment displacements toward the backfill area at integral frame bridges are caused by changes of length at the bridge structure due to temperature fluctuations. This allows the earth pressure to decline to the active earth pressure in winter, whereas in summer, the at-rest earth pressure is exceeded and the passive earth pressure is partly mobilised. Therefore, the changing earth pressure stress must be considered realistically for the entire period of use.

In order to verify Vogt's approach, which is currently used in Germany, earth-pressure measurements were carried out at different kinds of backfilling at a bridge near Frankfurt/Main over a period of almost three years. The structure was made of reinforced concrete and had shallow foundations. The deformations are influenced by the temperatures in the centre of the bridge superstructure. The performed measurements were able to prove that the temperatures at the bridge's centre can be well approximated by the average air temperature of the previous six days.

Due to the clear width between the abutments of 17.5 m, horizontal deformations between summer and winter position amounted to 4 mm. They caused considerable fluctuations of the measured earth pressure at backfill area 1 with coarse-grained soil between summer and winter, which were additionally superimposed by distinct daily fluctuations, while the biggest seasonal earth pressure fluctuations appeared at the earth pressure cells 4.3 m below the road surface (approximately half of the abutment's height). Their readings lay between 120 kN/m² in summer and 20 kN/m² in winter. The maximum daily fluctuations could reach 25 kN/m² and occurred mostly in summer.

The upper earth pressure cells showed an increase of the maximum readings over the three summers monitored so far, while the lower earth pressure cells revealed a reverse trend. Cohesion of the used material led to no earth pressure occurring until a depth of 2.5 m in winter. The ratio between the resulting earth pressure over the whole height of the abutments and the vertical stress declined to $K_{winter} = 0.23$. On the opposite, the resulting earth pressure in summer increased notably beyond the at-rest earth pressure and reached ratios of $K_{summer} = 0.96$.

Vogt's approach could be confirmed for the case that the total displacements between summer and winter position are used for the horizontal deformations.

By applying a vertical EPS layer at the earth side face of the abutment, the earth pressure stress at backfill area 3 could be reduced as it was aimed at.

The settlements of approx. 3 mm at the road surface and inside the backfill material were very small. The height divergences during implementation of the surface layer however could reach 20 mm. Therefore, inaccuracies during construction made up the main share of the measured unevenness in the longitudinal profile.

We would like to express our thanks to the Saxon Motorway Authority as well as to the Hessian Road And Traffic Administration for their cooperation. We also thank the German Federal Ministry of Transport, Building and Urban Development BMVBS represented by the Federal Highway Research Institute BASt for supporting this research project.

REFERENCES

1. Dicleli, M.; Erhan, S. (2010). Effect of soil-bridge interaction on the magnitude of internal forces in integral abutment bridge components due to live load effects. Engineering Structures, 32 (1): pp 129-145.
2. Engelsmann, S.; Schlaich, J.; Schäfer, K. (1999). Entwerfen und Bemessen von Betonbrücken ohne Fugen und Lager. Deutscher Ausschuß für Stahlbeton; Heft 496; Berlin.
3. England, G.L.; Tsang, N.C.M.; Bush, D.I. (2000). Integral bridges a fundamental approach to the time temperature loading problem; London.
4. Forschungsgesellschaft für Straßen- und Verkehrswesen (2009). Zusätzliche Technische Vertragsbedingungen und Richtlinien für Erdarbeiten im Straßenbau (ZTV E-StB 09); Köln.
5. Gebert, G.; Püchsel, J.-P.; Fitzenreiter, P. (2004). Musterentwürfe für Rahmenbrücken in Verbundbauweise und deren Umsetzung in der Praxis. Bauingenieur, 79 (4): pp 357-367.
6. Hoppe, E.J.; Gomez, j.P. (1996). Field Study of an Integral Backwall Bridge. Virginia Transportation Research Council; Charlottesville.
7. Kim, W.; Laman, J.A. (2010). Numerical analysis method for long-term behavior of integral abutment bridges. Engineering Structures, 32 (8): pp 2247-2257.
8. Kudla, W.; Szczyrba, S. (2010): Verformungen und Erddruck bei Widerlagerhinterfüllungen von integralen Brücken - neueste Messergebnisse und Ausführungsempfehlungen, in Proceedings Baugrundtagung in München, pp 155-162.
9. Pelke, E.; Berger, D.; Graubner, C.-A.; Zink, M. (2003). Fugenloses bauen, Entwurfshilfen für integrale Straßenbrücken. Schriftenreihe der Hessischen Straßen- und Verkehrsverwaltung; Heft 50, Wiesbaden.
10. Szczyrba, S.; Kudla, W. (2008). Setzungsreduzierende Bauweisen für den Hinterfüllbereich von Brückenwiderlagern, in Proceedings Baugrundtagung 2008 in Dortmund, pp 95-102.
11. Tsang, N.C.M.; England, G.L.; Dunstan, T. (2002). Soil/Structure interaction of integral bridge with full height abutments. in 15th ASCE Engineering Mechanics Conference. New York.
12. Vogt, N. (1984). Erdwiderstandsermittlung bei monotonen und wiederholten Wandbewegungen in Sand. Mitteilungen des Baugrundinstituts Stuttgart; 22; Stuttgart.